



Optical interferometry — A brief introduction

Markus Schöller

European Southern Observatory, Casilla 19001, Santiago 19, Chile

May 31, 2003

Abstract. Optical interferometry is an evolving field that in the current decade will become a tool for a wider astronomical community. We take a look at the principle underlying interferometry, introduce the key elements of an interferometer with examples from the VLT Interferometer, explain some constraints for interferometric observations and give an overview about the science which can be done with optical interferometers. While on this path we will try to illustrate several terms which are widely used by interferometrists.

Key words. Optical Interferometry, Very High Angular Resolution

1. Introduction

Interferometry between separate telescopes gives access to angular resolution which is much better than any single telescope can deliver. Interferometry is routinely operating at radio wavelengths since about 30 years, combining telescopes on different continents and even in space. During the same period optical interferometry went through a phase of definition and testing of the technology needed and produced science results regularly throughout the 1990s. The current implementation of larger facilities will bring optical interferometry into the astronomical mainstream.

There are ten optical interferometers in operations today: CHARA (ten Brummelaar et al. 2003), COAST (Haniff et al. 2003), GI2T (Mourard et al. 2003), IOTA (Traub et al. 2003), Keck (Colavita & Wizinovich 2003), MIRA (Nishikawa 2003), NPOI (Mozurkewich et al. 2003), PTI (Lane et al. 2003), SUSI (Tango

2003) and VLTI (Glindemann et al. 2003). Several more went out of service. Although they are very different in their design (e.g. they have telescope sizes between a few cm and more than 10 m), the wavelength regime they operate in (between 400 nm and 20 μ m), the modes of operation (pure visibility measurements, closure phases, phase referencing, wide and narrow angle astrometry, nulling), they all utilize the same underlying physical principles and use similar hardware. When we talk about optical interferometers in this paper, we think of interferometers which work at visible, near- or mid-infrared wavelengths and make a direct detection of fringes.

For a good overview about the status of optical interferometry in general, the reader is referred to Quirrenbach (2001) and for the historic context to Shao & Colavita (1992). An introduction into the key technology of optical interferometers has recently been presented by Schöller (2003). Information on

projects and resources within stellar interferometry can be found in the Optical Long Baseline Interferometry News under <http://olbin.jpl.nasa.gov/>.

2. Interferometers and interference

Optical interferometry – the coherent combination of the light from several telescopes at visible or infrared wavelengths – offers angular resolution far superior to that of a single aperture.

The angular resolution capabilities of an optical element are determined by its diameter D and the wavelength λ through λ/D . With a 10,cm telescope at 500 nm one can resolve structures as small as 1,arc-second. With a 10,m telescope the angular resolution is 10 milliarcseconds (mas), exactly 100 times better. If one wants to obtain even higher angular resolution, one has to build an even larger optical device, yet current telescope technology is preventing larger single aperture sizes.

In an optical interferometer, the angular resolution is given by λ/B , with B the distance between two telescopes, also called the baseline.

The principle of an optical interferometer can be best illustrated by Young's pinhole experiment, which is displayed in Fig. 1. A light source at infinity produces a flat wavefront which is passing through two holes which are separated by a distance B . On the screen behind these two holes, an interference pattern proportional to $1+\cos$ can be observed, with a period length of λ/B . This interference pattern is also called a fringe. The fringes disappear if the optical path difference (OPD – here: αB) is larger than the coherence length. The envelope of the fringe pattern is determined by the Fourier transform of the spectrum of the source modified by the optical filters used. With a light source under an inclination angle the fringe pattern shifts. The spacing of the fringes is solely determined by the spacing of the pinholes. If the source is resolved, the contrast of the fringes is diminishing, as several, respectively slightly shifted, fringe

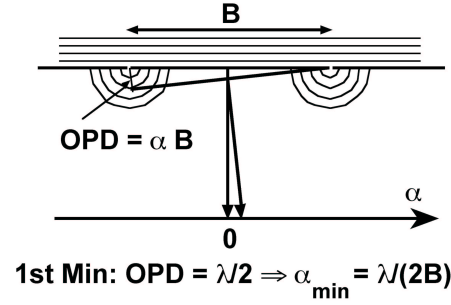


Fig. 1. Young's pinhole experiment.

patterns are adding up, smearing out the maxima and minima.

An interferometer is similar to masking a large telescope with just two pinholes. Changing the distance and the orientation between the two pinholes, one can slowly retrieve every single spatial frequency that a full aperture naturally gives in one instance. When observing with the full unmasked aperture, one gets an interferogram which has fringes between all subapertures. We call this also an image.

Fig. 2 shows the implementation of the VLT Interferometer. Instead of having just a screen with two holes, the light is following a complicated optical path. The main difference between the screen and a real setup is that the distance between the beams as they hit the telescopes and when they arrive within the beam combination device, is not the same anymore. The contrast of the fringes is determined by the resolution of the interferometer, i.e. the distance between the single apertures. The fringe spacing is solely determined by the distance of the beams in the laboratory.

The incoherent imaging equation describes the transfer function of an optical system as the autocorrelation of the pupil function. The transfer function is located in the Fourier space, or as interferometrists like to call it, the uv -plane, after the widely adapted names for its coordinates. In an interferometer with telescopes fixed to the ground the projected baselines change with the rotation of the earth. The baseline vec-

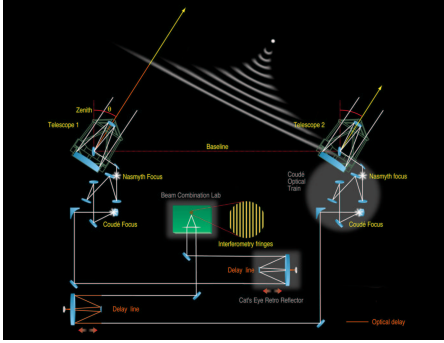


Fig. 2. The optical layout of the VLTI with two telescopes. The light is transported via a Coudé train to the Coudé focus and from there via relay optics into a tunnel which houses the delay lines. Finally, the light is sent into the interferometric laboratory where it is combined in an interferometric instrument.

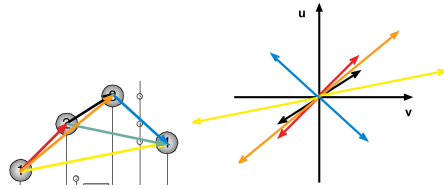


Fig. 3. The left image shows the VLTI with its four 8 m Unit Telescopes and the six baselines spanned by them. The right image shows the uv -coverage determined by this layout for an object located at zenith.

tors follow trajectories which are ellipses whose location is determined by the declination of the source and the latitude of the position of the interferometer. These ellipses become circles for objects with a declination of $\pm 90^\circ$ and degenerate to lines for objects with a declination of 0° . Fig. 3 shows the layout of the VLTI and a snapshot of the uv -plane for an object at zenith.

An interferometer measures visibilities. A visibility is a complex entity, the Fourier transform of the object intensity distribution, measured at the spatial frequency determined by the entrance pupil of the interferometer. The modulus of the visibility is determined by the contrast of the fringes, the phase of the visibility by the position

of the fringe. The contrast of a fringe is affected by the atmosphere and the interferometer itself. It has to be calibrated by an unresolved source, which has a visibility of 1. The fringe position is influenced mainly by the atmospheric turbulence, namely by the piston term. This effect can not be directly measured or calibrated. Phase information, which is the key to interferometric imaging, can be retrieved either through closure phases or through phase referencing. Closure phases are the sum of three simultaneously measured phases on three baselines which span a triangle. Closure phases are not influenced by atmospheric turbulence. Referenced phases are determined between a science object and a nearby unresolved source. They are usually retrieved with a dual feed system.

For a deeper understanding of the imaging process by means of Fourier optics, the reader is referred to Goodman (1968).

3. Ingredients of an interferometer

For an interferometer to work, the following components are sufficient: two telescopes, a beam combiner and the optical trains to tie them together. Most interferometers have telescopes which are fixed to the ground, and thus need delay lines to compensate for the OPD between the arms of the interferometer, while the source moves across the sky.

3.1. Telescopes

The main task of the interferometric telescopes as in any single aperture operation is to collect photons. A rigid design is needed to avoid any introduction of optical path difference due to vibrations, as for all components of the interferometer. As a golden rule, all telescopes of an interferometer should be of the same type, with the same orientation of mirrors and the same coatings on all conjugating optical surfaces to control differential polarization.



Fig. 4. Two delay lines of the VLTI.

3.2. Delay Lines

The delay lines have to compensate the OPD for all baselines in an interferometer. To do this, they have to cancel the OPD at any given time, i.e. follow the sidereal delay while the object moves across the sky.

The optics of delay lines are typically either a roof mirror or a cat's eye. Delay lines can be moved in various ways, with linear motors, voice coils or piezos. Typically they consist of a composition of these components, e.g. a linear motor for the coarse and a piezo for the fine positioning. This mix of devices makes it possible to achieve the positioning requirements of the delay lines with an accuracy of tenths of nanometers over a stroke length of tenths of meters.

Fig. 4 shows the implementation of the VLTI delay lines.

3.3. Beam combination

A beam combiner brings the beams from the telescopes close enough together so they can interfere. If the beam combination scheme requires the coding of the fringes in time, a device to modulate the OPD between the beams is required. Further, some type of detector to record data is needed.

There are two different ways to combine beams in a beam combiner: in a multi-axial beam combiner the beams are placed adjacent to each other and form a fringe pattern in space. In a coaxial beam combiner, the beams are added on top of each other, for

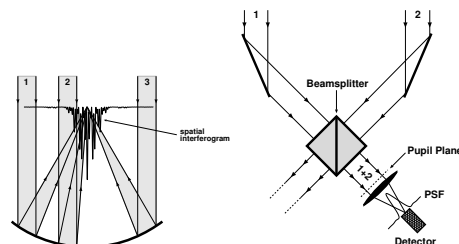


Fig. 5. Fringe combination schemes: multi-axial (left) and coaxial (right). An OPD modulating device has to be used in one of the arms of the coaxial beam combiner to form fringes.

example with a beam splitter. The fringes are produced in time by modulating the OPD between the two beams. Fig. 5 illustrates the two combination schemes and in Fig. 6 one can see the data resulting from the beam combination.

The actual implementation of a beam combiner is usually done in bulk optics. Another type of beam combiner is made out of single mode fibers, which are not only combining the light within the fibers, but also serve as spatial filters (Coude du Foresto et al. 1993). Lately, progress in the production of integrated optics has allowed to build beam combiners of the size of a coin (Malbet et al. 1999; Berger et al. 2001).

3.4. Further components

Since the light of two (or more) telescopes has to be combined, it is necessary to bring their light onto the same spot in an image plane. Tip-tilt sensors for each telescope are employed to ensure the image stability needed. If the telescopes are larger than the diameter of the atmospheric turbulence cells (the Fried Parameter r_0), then the telescopes have to be equipped with adaptive optics to ensure the maximum flux being available for beam combination. A spatial filter ideally removes residual inhomogeneities of the individual wavefronts (and thus makes them similar), at the cost of reducing the amount of light which is avail-

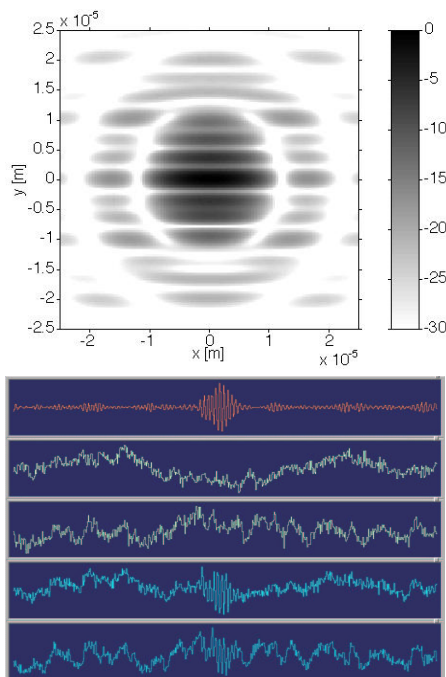


Fig. 6. The fringes resulting from multiaxial and coaxial beam combination: on the top a simulation of fringes similar to the ones which will be produced by the AMBER instrument on VLTI is presented. The bottom panel displays fringes observed by the VINCI instrument on VLTI.

able for beam combination. Finally, a fringe tracker stabilizes the fringes, which are otherwise moved backwards and forwards in OPD by the atmospheric piston.

4. Observing with optical interferometers

Optical interferometers have two limitations which have to be taken into account when looking for the science cases they can tackle: a limited field of view and a relatively poor limiting magnitude.

The field of view is limited to a few arcseconds due to the transfer optics that bring the light from the telescopes to the beam combination device. A larger field of view would require larger optical elements. Furthermore, beam combination devices of-

ten use spatial filters, which are adapted to the Airy disk of a diffraction limited telescope. High resolution information can then only be retrieved within this field, which is e.g. 55 mas for an 8 m telescope at $2.2 \mu\text{m}$. Information is sampled only on B/D resolution elements, which e.g. corresponds to $130 \text{ m}/8 \text{ m} \approx 16$ elements for the VLTI 8 m telescopes or $220 \text{ m}/1.8 \text{ m} \approx 112$ elements for the 1.8 m telescopes. Ways to overcome these field of view limitations are mosaicing and homothetic mapping, which both have not been successfully implemented on optical interferometers yet.

The limiting magnitude is determined by the atmosphere moving the fringes back and forth due to the piston term. Interferometers have to beat this motion, limiting the integration time to the atmospheric coherence time τ_0 . Apart from building an interferometer at an exceptional site with a large τ_0 , one can overcome this limitation by using large telescopes with adaptive optics to collect more photons and use off-axis fringe trackers in dual feed systems. A limiting magnitude in the K band of about 20 is within reach of the existing large interferometers.

The most simple interferometric observations are of rotationally symmetric objects, like diameter measurements of stars. Fig. 7 shows such observations for α Cen A and B. Each obtained (squared) visibility value is plotted against the baseline length (or the spatial frequency) and a model fit is made to the data, here a uniform disk diameter. It is possible to find asymmetries from visibilities without phase information, but there is always a 180° ambiguity. With interferometers which allow to obtain more information, more complex models can be fitted. Especially phase information allows to distinguish between different models and finally permits imaging. Yet, although there are optical interferometers which are regularly measuring closure phases, not a single model independent image has been retrieved so far.

The classical field of optical interferometry is the determination of fundamental

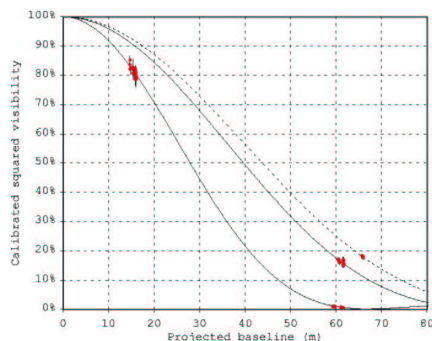


Fig. 7. Visibility values and the resulting uniform disk fits for the three stars α Cen A (lower solid curve), α Cen B (upper solid curve) and θ Cen (dashed curve – the calibrator used). The derived uniform disk diameters are 8.338 ± 0.018 mas and 5.905 ± 0.045 mas for α Cen A and α Cen B, respectively (see Kervella et al. 2003).

stellar quantities, like the diameter, limb darkening profiles or asymmetries. Surface structures on stars should become accessible in the future with longer baselines. Another field are binarity studies, especially in star forming regions. Other topics of interest are stellar environments like stellar debris disks, circumstellar disks and jets of pre-main sequence stars, or mass outflows of evolved stars. Finally, the two big challenges for optical interferometry are the detection of extrasolar planets (see e.g. Glindemann et al. (2000) for an overview of available techniques) and the observations of active galactic nuclei, the first extragalactic sources for optical interferometry. Since optical interferometry is improving angular resolution by more than one magnitude over what is available with single telescopes, the history of astronomy tells us that we can expect to find a wide variety of new phenomena.

Acknowledgements. I would like to thank the whole interferometric community for fruitful

discussions over the years, especially the people in the VLTI group at ESO. Pierre Kervella kindly provided the figure on α Cen.

References

- Berger, J.P., P. Haguenauer, P. Kern, et al. *A&A*, 376:L31, 2001.
- Colavita, M.M. and P.L. Wizinovich *SPIE* 4838, 625, 2003.
- Coude du Foresto, V., G. Maze, and S. Ridgway. *ASP Conf. Ser.* 37:285, 1993.
- Glindemann, A., F. Delplancke, P. Kervella, et al. *In: Planetary Systems in the Universe*, IAU Symp. 202, 2000, Ed. A.J. Penny, P. Artymowicz, A.-M. Lagrange, S.S. Russell, 2000
- Glindemann, A., J. Argomedo, R. Amestica, et al. *In: The Very Large Telescope Interferometer: Challenges for the Future*, Ed. P.J.V. Garcia, A. Glindemann, Th. Henning, F. Malbet, *in print*, 2003.
- Goodman, J.W. *Introduction to Fourier Optics*, McGraw-Hill, 1968
- Haniff, C.A., J.E. Baldwin, A.G. Basden, et al. *SPIE* 4838, 19, 2003.
- Kervella, P., Thévenin, F., Ségransan, D., et al. *A&A accepted*
- Lane, B.F., M. Konacki, and R.R. Thompson *SPIE* 4838, 62, 2003.
- Malbet, F., P. Kern, I. Schanen-Duport, et al. *A&AS*, 138:135, 1999.
- Mourard, D., L. Abe, A. Domiciano, et al. *SPIE* 4838, 9, 2003.
- Mozurkewich, D., J.A. Benson, and D.J. Hutter *SPIE* 4838, 53, 2003.
- Nishikawa, J. *SPIE* 4838, 101, 2003.
- Quirrenbach, A. *Annual Review of Astronomy and Astrophysics*, 39:353–401, 2001.
- Schöller, M. *In: The Very Large Telescope Interferometer: Challenges for the Future*, Ed. P.J.V. Garcia, A. Glindemann, Th. Henning, F. Malbet, *in print*, 2003.
- Shao, M. and M.M. Colavita. *Annual Review of Astronomy and Astrophysics*, 30:457–498, 1992.
- Tango, W.J. *SPIE* 4838, 28, 2003.
- ten Brummelaar, T.A., H.A. McAlister, S.T. Ridgway, et al. *SPIE* 4838, 69, 2003.
- Traub, W.A., A. Ahearn, N.P. Carleton, et al. *SPIE* 4838, 45, 2003.